DIFFUSE X-RAY SCATTERING STUDY OF DEFECTS CREATED BY keV ION IMPLANTS IN Si

P.J. PARTYKA *, R.S. AVERBACK *, K. NORDLUND *, I.K. ROBINSON *, D. WALKO *,
P. EHRHART **, T. DIAZ de la RUBIA ***, M. TANG ***
*Materials Research Laboratory, University of Illinois at Urbana, Urbana, IL
**Institut für Festkörperforschung, Forschungszentrum Jülich, Jülich, Germany
***Lawrence Livermore National Laboratory, Livermore, CA

ABSTRACT

Diffuse x-ray scattering (DXS) and computer simulation techniques were employed to investigate the defect structure produced in Si by low keV ion and MeV electron irradiations. DXS measurements were performed for keV Ga and He implants, demonstrating the ability of the technique to provide both bulk and near-surface measurements at defect concentrations of about 1000 ppm. A rigorous analysis of these results is complicated due to the complex nature of the ion damage in Si. A computer simulation framework is developed to aid in the analysis of this data. In this technique, defects are simulated and their strain fields are calculated by simply relaxing the atoms around the defect to their equilibrium positions. The diffuse scattering is then calculated from the strain field, and the results are compared to the experimental measurements. Computer simulations are presented here only for the case of electron irradiation damage and compared to published measurements.[1] Application of the technique to more complicated structures is planned and should pose no serious problems in the computational framework already developed.

INTRODUCTION

The goal of this work is to develop a method for identifying small defects created in the early stages of the ion implantation process in Si. Clearly, understanding this early stage is crucial to understanding all subsequent stages of the defect formation process, but little information is currently available about this stage as most techniques are insensitive to these small defects or are unable to identify their exact nature. The DXS technique is capable of examining low concentrations of both deep and shallow implants as both the diffuse scattering measurements and the simulations can be applied to investigate defects which lie as deep as several microns from the surface or as shallow as under 10 nm.

Since the theory of the diffuse scattering from crystalline defects is well developed, only the most relevant highlights will be presented.[2-7] Huang first calculated the diffuse scattering from point defects modeled as perfect centers of dilation in an isotropic medium.[2] The resultant diffuse scattering is expressed as

$$I_{defect} \propto c \cdot \Omega_{rel}^{2} \cdot \left(\frac{|\vec{K}|^2}{|\vec{q}|^2} \right) \qquad (1)$$

Here c is the defect concentration, Ω_{rel} is the defect relaxation volume, $\vec{K}$ is the scattering vector, and $\vec{q}$ is the difference vector of $\vec{K}$ and $\vec{G}$, where $\vec{G}$ is the nearest reciprocal lattice vector. Later work showed that the introduction of anisotropy in cubic crystals (either from the defect or from the lattice constants or from both) does not fundamentally alter this dependence, but simply gives the scattering an additional dependence upon the direction of $\vec{q}$, or equivalently upon the scanning direction in reciprocal space.[3] This directional dependence is important because it essentially contains information about the strain field of the defect. Thus, by measuring the scattering intensity along different directions in reciprocal space, information about the defect configuration is obtained.

Mat. Res. Soc. Symp. Proc. Vol. 439 © 1997 Materials Research Society

The diffuse scattering technique has been applied with great success to the study of simple defects in pure metals.[4-6] Point defect concentrations at the level of hundreds of ppm and defect relaxation volumes have been measured, and defect configurations have been identified. Additionally, it has been shown that clusters of defects and even simple dislocation loops can be specifically recognized.[6] Yet application of the technique to semiconductors is more complicated for several reasons.

First of all, a simplification which arises in the metals does not arise in the semiconductor systems. In both systems, when a point defect is created by ejection of an atom from its lattice site, there are two parts to the defect, the interstitial and the vacancy. This close pair defect is stable and is created in both systems, but in metals the diffuse scattering due to the defect is dominated by the interstitial contribution. This is because the vacancy relaxation volume in metals is small and so is its scattering intensity can be neglected. For semiconductors, the interstitial and vacancy have similar relaxation volume magnitudes, and thus both contribute significantly to the diffuse scattering.[1] Analysis of the scattering will potentially yield information about the interstitial, the vacancy, and their relative average configuration, but may be difficult, and it should be remembered that this is the simplest possible defect.

Another complication in semiconductors is that cascade damage is often very complex. Unlike metals, cascade damage may not collapse to point defects or clusters of point defects, but may result in highly disordered or even amorphous zones involving many atoms. Thus, identifying defects and modeling their structure is difficult.

A final complication in semiconductors is associated with measuring damage very near the surface, as is produced by keV ion implantations. Sensitivity to such shallow damage requires the use of glancing geometries for the x-rays at a brightness available only at synchrotrons. Additionally, the modeling of shallow defects is complicated by the possible effects of the surface on the defect.

The difficulties of defect complexity can be reasonably approached by computer modeling. A molecular dynamics (MD) simulation can efficiently relax possible defect structures, and the scattering resulting from the associated strain field can be calculated and compared to experimental observations. Additionally, the defect structures themselves can be 'guessed' by simulating the passage of energetic ions through the material. The complexity of the defect is unimportant as the calculation is based simply on energy minimization. Also, complications such as surfaces can be added without much difficulty. In such a manner, implantation defects can be modeled and compared to experiments.

EXPERIMENT

For this study phosphorous doped (25-56 Ω-cm), Cz grown Si (111) wafers with low miscut angles (< 0.1) were used. Before implantation, the native oxide was removed using an HF etch. The samples were then mounted on a cryogenic diffractometer which was part of a high vacuum chamber at beamline X16A at the National Synchrotron Light Source at Brookhaven National Laboratory. Samples were examined in situ before implantation, at a series of doses during implantation, and after thermal annealing. Implantations were performed at -50 C and at 20 C. Implants were performed using either a 5 kV differentially pumped gas source ion gun using He^+ at 4.5 kV or a 25 kV liquid metal source ion gun using Ga^+ at 20 kV. Samples were examined using x-rays with a wavelength of 0.11262 nm and a position sensitive detector was employed. Radial and transverse scans were performed near bulk Bragg peaks, both in the surface plane and out-of-plane. Glancing angles as small as 0.2° were used to enhance surface sensitivity.

Computer simulations were used to model the diffuse scattering from defects in Si. Defect configurations were deduced using MD simulations in a periodic boundary cell. The defect was then relaxed to a larger cell size of about 1 million atoms using a conjugate gradient method. Extrapolation of the strain field to yet larger cells of up to 25 million atoms was performed in a separate final routine. Once the atomic positions were obtained, the diffuse scattering was calculated and compared to experimental observations.[8] Presently, comparison only to electron irradiation results published by Ehrhart et al have been made.[1] Extension to more complicated defects and to defects near surfaces is underway and should be straightforward.

RESULTS AND DISCUSSION

Results are presented here in order of increasing complexity. First, as a test of our technique, scattering calculations from a defect simulated in Cu are compared to the scattering calculated by other methods for the actual defect in Cu, which has been identified as the [100] dumbbell interstitial by diffuse x-ray scattering measurements.[4-5] By visual inspection, we first verified that the simulation algorithm produced the same [100] dumbbell interstitial as found in the real crystal. Next a comparison of iso-intensity contours from the simulated defect and from analytical expressions for the real defect was performed, as shown in Figures 1a and 1b. Finally, the q dependence of the intensity in the radial [100] and the transverse [001] directions was calculated for the simulation and is shown in Figure 2. The radial scan produced an expected q^{-2} dependence, while the transverse scan showed much lower scattering and essentially no q dependence.

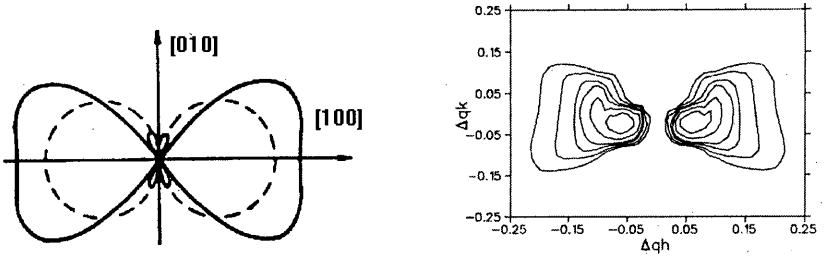

Figure 1. Calculations for the [100] dumbbell interstitial in Cu at the (200) peak. Figure 1a shows the spherical iso-intensity contours derived from Huang's isotropic defect and a lemniscate due to the actual configuration as calculated by Dederichs.[4-5] Figure 1b shows the contours calculated by the present method. The x and y axes correspond to the [100] and the [010] directions in reciprocal space, and the units are in terms of the reciprocal of the Cu lattice parameter.

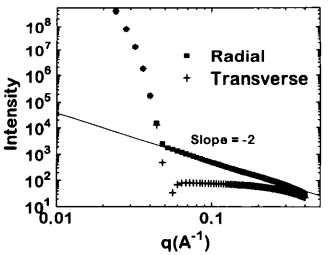

Figure 2. The q dependence of the scattering intensity is shown for the simulated [100] dumbbell interstitial in Cu in the radial and transverse directions. The simulated results match experimental measurements with a q^{-2} radial dependence and a zero intensity line in the transverse direction.

All the simulations of the Cu defect are consistent with the experimental data. The shape of the iso-intensity contours of the simulation (1a) matches the experimental defect (1b), although the exact shapes differ slightly. These differences are thought to be due to shortcuts we took to limit computational time. These include limiting the number of atoms in the cell and the fineness of the grid and ignoring the subtraction of the scattering of the perfect lattice, which has a small contribution compared to the defect in most directions. The q^{-2} dependence and the zero intensity plane found in experiments are reproduced well by the simulation in Figure 2.

Satisfied with the results in Cu, we next compare experimental measurements from Ehrhart of defect scattering after 2.5 MeV electron irradiation of Si at 4K to a simulated defect in Si.[1] The

simulated defect was shown to be stable in MD simulations.[9] It is a point defect with a relaxation volume ≈ 0, and thus is a candidate for being the defect caused by electron irradiation which also is known to have a formation volume ≈ 0.[1] Figure 3a plots the experimental scattering intensity multiplied by q^2 vs q/G in the radial direction at the (511) peak while Figure 3b shows the corresponding simulation results. Note that the q axis in each has a different scale by a factor of about 6. Plotting the data in this manner should yield a horizontal line for the q^{-2} dependence found in Huang scattering. Such a line is drawn as a guide to the eye.

Although the shape of the scattering is similar in both figures, the scale of q is much different. This indicates that while the defects causing the scattering have some similarities, they also have important differences. The shape of both is consistent with scattering from a defect pair whose total relaxation volume ≈ 0. The difference in the q scale indicates that the separation of the interstitial and the vacancy parts of the defect are different for the real and simulated defects. The simulated defect has a very small separation of the defect pair (< the nearest neighbor distance) which causes the deviation from the q^{-2} dependence to occur at large q values. For the real defect, the deviation from the q^{-2} dependence occurs at a much smaller q, indicating that the average separation of interstitial and vacancy in the real crystal is much larger than that of the simulated defect (by a factor of 5-6). Thus, we can say with confidence that the real defect responsible for the experimental diffuse scattering is not the simulated defect. To gain information about the possible existence of the simulated defect in the real crystal, another measurement is needed to be taken at larger q values. The current small q measurements are not at all sensitive to the simulated defect; thus, we cannot conclusively answer at this time whether or not it exists in real Si. Attempts to simulate other possible defects in electron irradiated Si are underway and will consider defects with larger separations.

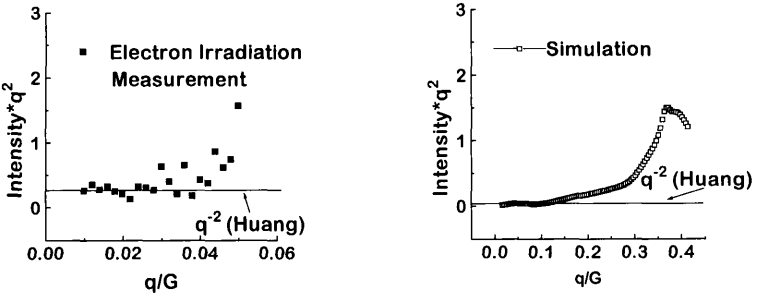

Figure 3. Figure 3a shows the diffuse scattering caused by 1 MeV electron irradiation of Si measured in the radial direction at the (511) peak at 4K by Ehrhart et al.[1] Figure 3b shows the calculated scattering from a simulated defect thought to be a possible defect created by such electron irradiations. Although the shapes of both curves are similar, the scale in q is much different, showing that the scattering in each is caused by different defects with large differences in the separation of the interstitial-vacancy pair.

The goal of this project is to identify defects in low keV ion implanted Si. Shown in Figures 4a and 4b are measurements for such implants. The data shown are from samples implanted with 20 keV Ga^+ at room temperature and with 4.5 keV He^+ at -50 C, respectively. The samples were examined at the (422) peak in the radial direction under a glancing geometry employing entrance and exit angles of 0.2° to enhance surface sensitivity, since the implantations penetrated only 30 nm (Ga) and 100 nm (He). The bottom curve in each shows the scattering from the unimplanted crystal, which is eventually subtracted from the implanted data to eliminate scattering sources such as thermal vibration and Compton and inelastic scattering. Sensitivity limits of defect scattering in both cases correspond to doses of $\approx 2 \times 10^{-3}$ dpa which is about 1/100 of the dose for amorphization.[10] The defect scattering is seen to increase consistently with dose. It is noted that the Ga implant causes more scattering at the +q side of the peak

while the He implant is more symmetric, although this effect is hard to see on the logarithmic intensity scale. Figure 5 elucidates the effect more clearly.

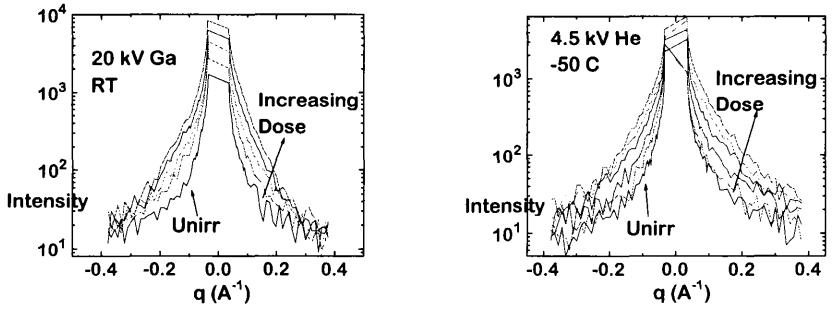

Figure 4. The scattering due to a 20 kV Ga implant at room temperature is shown in Figure 4a. Figure 4b shows the scattering from a 4.5 kV He implant at -50 C. Both data sets were taken in a glancing geometry at the (422) surface peak.

Some simple analysis of the data can already supply information about the nature of the implants. For the data sets shown, the symmetric and antisymmetric parts of the scattering (with respect to q) are plotted in Figures 5a and 5b respectively. Also shown in these figures is data from a similar implant of 4.5 keV He^+ performed at room temperature. This additional data was not shown earlier, but it is also noted to have more intensity at the +q side of the peak. The x axis of the figure normalizes for the different implant depths and thus the total number of defects by multiplying dpa by range.[11] From the initial slopes of the symmetric scattering, it is seen that the Ga implant is three times more efficient at creating damage than the room temperature He implant, assuming both implants cause similar clustering (which will be addressed next). This is consistent with similar efficiencies measured in ion channeling and in computer simulation studies.[12] The larger slopes of these implants as compared to the colder He implant suggest that both exhibit clustering as clusters are stronger x-ray scatterers than individual defects.[4-6] The anti-symmetric scattering supports this conclusion. The large positive anti-symmetric scattering indicates clustering of interstitials, while the small (≈0) antisymmetric scattering seen in the colder He implant indicates that clustering occurs much more slowly for these conditions. These

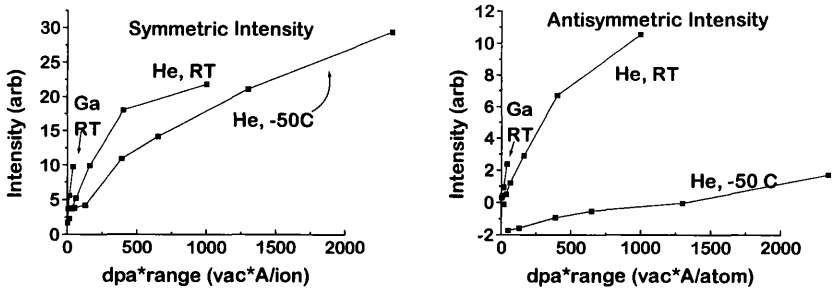

Figure 5. The symmetric intensity is plotted in 5a for three implants. The larger initial slope for the Ga implant is attributed to greater defect production efficiency. The difference between the He implants is attributed to clustering of defects in the room temperature implant. These conclusions are supported by the anti-symmetric intensity shown in Figure 5b. The similarity in slopes of the Ga and He RT data (to the symmetric data) indicate that the clusters are of similar size, while the low value for the colder He implant indicates reduced clustering. The clusters are thought to be interstitial clusters.

observations all appear consistent with the nature of cascade producing implantations vs non-cascade producing ones, and with the effect of temperature to enhance clustering.

Further information about the exact nature of defects created in these keV irradiations has not yet been deduced. Simulations are currently underway to investigate the possible defect structures involved. This includes simulating the passing of ions through a lattice to create the damage and simulating structures such as small (311) defects known to exist in Si after high dose implants.[13] These simulations can then be compared to the above experiments to try to identify the exact nature of the damage. Once this is done, the formation and concentrations of these defects could then be monitored as a function of dose or annealing.

CONCLUSION

In situ measurements were performed of the diffuse x-ray scattering from defects introduced into Si (111) by keV ion implants. These employed a glancing geometry and synchrotron radiation to achieve a point defect sensitivity of about 1000 ppm of defects in implants as shallow as 30 nm. A computational framework employing molecular dynamics simulations and conjugate gradient techniques was developed to simulate defects of arbitrary complexity and their expected diffuse scattering. This simulated scattering can be compared to experimental results to identify defect configurations in actual implantations. Examples were calculated for a known defect in Cu and for a possible defect in electron irradiated Si and compared to experimental results.

ACKNOWLEDGMENTS

This work was performed at the University of Illinois under DOE grant DEFG02-91ER45439, at Brookhaven National Laboratory under DOE grant DEAC012-76CH00016, at Lawrence Livermore National Laboratory, and at the Institut für Festkörperforschung, Forschungszentrum Jülich, Germany.

REFERENCES

1. St. Bausch, H. Zillgen, P. Ehrhart, Mat. Sci. For. **196/201**, p. 1141 (1995).
2. K. Huang, Proc. Roy. Soc. (London) **A190**, p. 102 (1947).
3. H. Trinkaus, Phys. Stat. Sol. (b) **51**, p. 307 (1972).
4. P. H. Dederichs, Phys. Rev. B, **4**, p. 1041 (1971).
5. P. H. Dederichs, J. Phys. F, **3**, p. 471 (1973).
6. P. Ehrhart, H. Trinkaus, B.C. Larson, Phys. Rev. B, **25**, p. 834 (1982).
7. H. Kanzaki, J. Phys. Chem. Sol., **2**, pp. 24,107 (1957).
8. D. T. Keating, A. N. Goland, Acta Crytstallogr. **A27**, p. 134 (1971).
9. M. Tang, L. Columbo, J. Zhu, T. Diaz de la Rubia, submitted to Phys. Rev. B.
10. C. A. Volkert, A. Polman, Mat. Res. Soc. Symp. Proc., **235**, p. 3 (1992)
11. J. Ziegler, J.P. Biersack, U. Littmark, Stopping and Range of Ions in Solids, Pergamon, NY, 1985, Vol 1.
12. M. J. Caturla, T. Diaz de la Rubia, L. A. Marqués, G. H. Gilmer, submitted to Phys. Rev. B.
13. D. J. Eaglesham, P. A. Stolk, H. J. Gossman, T. E. Haynes, J. M. Poate, Nucl. Inst. Meth. Phys. Res. B, **106**, p. 191 (1995).

This article also appears in Volume 438.